Electrical Power and Energy Systems 101 (2018) 38–49

Contents lists available at ScienceDirect

Electrical Power and Energy Systems

journal homepage: www.elsevier.com/locate/ijepes

An improved control for simultaneous sag/swell mitigation and reactive power support in a grid-connected wind farm with DVR

S. Priyavarthini[a], C. Nagamani[a], G. Saravana Ilango[a,*], M.A. Asha Rani[b]

[a] Department of Electrical and Electronics Engineering, National Institute of Technology, Tiruchirappalli, India
[b] Department of Electrical and Electronics Engineering, Madanapalle Institute of Technology and Science, Chittoor, India

ARTICLE INFO

Keywords:
Dynamic Voltage Restorer (DVR)
Fault Ride Through (FRT)
Fixed Speed Wind Generator (FSWG)
Reactive power support
Sag/swell mitigation
Phase Angle (PA) control

ABSTRACT

Commonly a Dynamic Voltage Restorer (DVR) is installed to protect a wind farm from grid side disturbances, voltage sag/swell, or for riding through low voltage or fault. This work proposes a novel technique to utilize the DVR to compensate the reactive power demand of the fixed speed wind generator apart from mitigating sag/swell in grid voltage. The voltage injected by the DVR is regulated so as to maintain a constant voltage at the generator terminals while the phase of the generator terminal voltage lags the grid voltage by a constant angle. The possibility of better utilization of DVR to compensate reactive power demand of Fixed Speed Wind Generators (FSWG) along with Fault Ride-Through (FRT), Sag/Swell mitigation is explored in this work by implementing 'Phase Angle'(PA) control in DVR. A comprehensive analysis is presented for the 'Phase Angle' control and the boundaries of operation for simultaneous reactive power supply and sag/swell mitigation are illustrated in graphical analysis. The effectiveness of the proposed 'PA' control scheme on simultaneous operation of sag/swell mitigation and reactive power compensation is verified using simulations in PSCAD/EMTDC for a 2 MW induction generator and also using laboratory tests on a 0.75 kW induction machine.

1. Introduction

Wind Energy Conversion System (WECS) is one of the rapidly developing renewable power generation systems all over the world [1]. However the integration of WECS to the grid is still a major issue due to the intermittent nature of wind, Power Quality (PQ) issues, capacitor switching, resonance, etc. Among all the PQ issues, the sudden dip in voltage at the wind generator terminal due to fault in grid side may lead to sudden tripping of FSWGs from the grid. The frequent tripping and reconnection of wind generators may severely affect the stability of the grid. In order to limit the tripping of wind generators from grid, several nations have developed new grid codes for grid connected WECS to maintain the stability of the grid during grid voltage abnormalities or faults [2]. The Indian Electricity Grid Code (IEGC) [3] demands certain constraints on the performance of the WECS such as maintenance of power factor in the range of ± 0.95, tolerance to grid voltage sag/swell of certain depth and faults. Low voltage ride-through was addressed [4] to effectively manage and interconnect the wind turbines to the grid.

Majority of WECS in India employ Squirrel Cage Induction Generators (SCIG) which operate as Fixed Speed Wind Generators (FSWGs) due to the simplicity, low cost and rugged operation. Owing to the sensitivity of FSWGs to grid voltage imperfections like voltage sag/swell, faults, sub-synchronous resonance (SSR), capacitor switching transients, special equipment are installed to ensure the compliance with the grid codes. Several compensators are proposed to protect FSWGs from various grid side disturbances to ensure stability of both wind generator and the grid. The STATCOM is utilized for Fault Ride Through (FRT) [5] and for asymmetrical faults mitigation in FSWGs [6]. A Combination of Series Dynamic Braking Resistor (SDBR) and STATCOM are employed to enhance the transient and dynamic stability of fixed speed wind farms [7]. The STATCOM with braking resistor and additional series impedance is shown to improve stability of fixed speed wind generators [8] while a series compensator is employed to mitigate SSR in FSWGs [9]. A Multi-Functional Series Compensator (MFSC) is proposed [10] to protect the FSWGs from grid side faults. The Unified Inter-Phase Power Controller (UIPC) [11] is proposed to improve stability under grid fault conditions with a modified control scheme and the operation is divided into normal and low-voltage ride through (LVRT) mode based on grid condition. A Controllable Resistive Type Fault Current Limiter (CR-FCL) is proposed in [12] for fault ride through (FRT) protection in a SCIG wind farm whereas an optimum value of resistance is inserted during fault to achieve maximum FRT. A bridge-type fault current limiter [13] was reported to improve fault ride-through capability of FSWGs while an optimal resistive type fault

* Corresponding author.
E-mail addresses: priya91gct@gmail.com (S. Priyavarthini), cnmani@nitt.edu (C. Nagamani), gsilango@nitt.edu (G.S. Ilango), asha_siju@yahoo.co.in (M.A.A. Rani).

https://doi.org/10.1016/j.ijepes.2018.03.016
Received 11 September 2017; Received in revised form 22 December 2017; Accepted 10 March 2018

current limiter is implemented to achieve maximum fault ride-though capability of FSWGs under symmetrical and unsymmetrical grid faults [14].

A review on active filters with grid connected fixed and variable speed wind generators is discussed in [15]. In [16], DVR is proposed to improve the FRT capability of SCIG based wind farms. Comparison of various compensation devices for FRT [17,18] for induction generators are revealed that the DVR (series compensator) renders a superior dynamic performance during fault conditions. Inclusion of a DVR facilitates FRT and Low Voltage Ride Through (LVRT) thus enhancing the stability of both grid and wind farm with FSWGs and DFIGs as discussed in [19–26].

Since the wind farms should maintain the power factor within the limit in order to satisfy the grid code, the reactive power demanded by FSWG is drawn from external capacitor banks. The switching of capacitor causes undesirable effects such as oscillatory transients, resonance in the electrical and mechanical subsystems in the grid [27,28]. The effects of resonance caused by the shunt capacitors and the voltage stress at wind terminal and subsequent tripping of the fixed speed wind turbine due to malfunction in capacitor switching are pointed out [29,30] and STATCOM integrated with switching capacitors yielded superior operation. In a similar approach, utilization of DVR to address the dual issues of reactive power support as well as mitigating the grid voltage imperfection both reactive power compensation and mitigation of voltage stress at the FSWG terminal is proposed. That is, the role of a DVR available in the wind farm for FRT/LVRT protection can be expanded to include the reactive power support thereby enhancing the value of the DVR. The voltage injected by the DVR is so regulated as to maintain a constant voltage at the generator terminals while the phase of the generator terminal voltage lags the grid voltage by a constant angle for constant power factor (due to fixed speed) of FSWG. Thus by controlling the phase angle between the generator and grid voltages, the DVR is commanded to supply the reactive power needed by the wind farm although the grid voltage fluctuates. The proposed concept is illustrated through a comprehensive phasor and graphical analysis. A DVR fed from the line via a Diode Bridge Rectifier (DBR) is chosen for this work [31]. Two test systems are considered for investigation; (i) A 2 MW wind farm (using SCIG) and a DVR and (ii) A laboratory set up with a 0.75 kW SCIG and a DVR. Computer simulations using PSCAD/EMTDC software validate the proposed control. Tests are also carried out on the laboratory system. Results establish the effectiveness of the proposed control.

In Section 2, the system description is discussed. The theoretical and graphical analysis of the proposed system is explained in Section 3. In Section 4, the phase angle control strategy for DVR is explained. The simulation and experimental validation of the proposed scheme is demonstrated in Section 5.

2. System description

The general system configuration of a DVR installed in a wind farm is shown in Fig. 1(a). The system consists of a series connected Voltage Source Inverter (VSI) and a shunt converter (Diode Bridge Rectifier) to charge the dc-link capacitor. The VSI output terminals are connected to an LC filter and to the grid through series transformer. A dc chopper is connected across the dc-link to limit the rise of dc-link voltage under power reversals. Generally the VA rating of DVR is selected based on the range of sag/swell needed to be mitigated in wind farm and in order to ride through faults, the DVR VA rating of 1.0 p.u. is installed in wind farms. Thus the DVR VA rating of 1.0 p.u. is considered for the analysis and simulations in the proposed work.

The theoretical and graphical analysis of the grid connected FSWG with a DVR is presented in the upcoming sections. The efficacy of the proposed "Phase Angle" control is analysed under different cases of grid voltage such as, Case 1: Nominal Grid Voltage, Case 2: Sag in Grid Voltage(symmetrical), Case 3: Swell in Grid Voltage(symmetrical), Case 4: Unsymmetrical grid voltage. The source convention is followed for grid and DVR whereas, load convention is followed for wind generator and shunt converter (DBR).

3. Theory of phase angle (PA) control in DVR

Various types of compensation methods for DVR as reported in [32] are effective only during grid side disturbances such as sag/swell, phase jump, fault, etc. and the DVR remains idle during nominal grid conditions. However, in the proposed scheme, the DVR is engaged continuously even at nominal grid voltage, functioning to meet the reactive power demanded by the FSWG. The proposed "Phase Angle" control scheme of DVR in FSWG is explained in this section. The 'PA' control is illustrated with phasor diagram as shown in Fig. 1(b). The grid voltage V_g is considered as the reference phasor. The terminal voltage V_t is represented to lag the grid voltage V_g by an angle δ whereas the line current is required to be exactly out of phase with grid voltage to maintain unity power factor irrespective of grid voltage variations.

Since in general the variation of rotor speed of a FSWG is only about 1–2% of rated speed [33], the FSWG is modelled as a fixed impedance in this work. Therefore at a given speed, the effective impedance and thereby the real and reactive power of the FSWG can be considered constant if the magnitude of terminal voltage is maintained constant. Thus from the Fig. 1(b), the phase angle δ between the terminal and grid voltage can be expressed as,

$$\delta = 180° - \varphi_w \tag{1}$$

By maintaining the phase angle δ constant, the unity power factor can be maintained at the grid. Thus the magnitude of the terminal voltage is maintained at the nominal value while the phase of $\vec{V_t}$ is also maintained constant at 'δ' with respect to the grid voltage.

From Fig. 1(b), the terminal voltage ($\vec{V_t}$) can be written as,

$$\vec{V_t} = \vec{V_g} + \vec{V_c} \tag{2}$$

From (2), the magnitude and phase angle of injected DVR voltage are given by,

$$|V_c| = \sqrt{(V_t cos\delta - V_g)^2 + (V_t sin\delta)^2} \tag{3}$$

$$\text{and } \theta_c = \tan^{-1}\left(\frac{V_t sin\delta}{V_t cos\delta - V_g}\right) \tag{4}$$

where θ_c is the injection angle of DVR and δ is the angle between grid and terminal voltage.

The grid current can be written as follows from Fig. 1(b),

$$\vec{I_g} = \vec{I_{sh}} + \vec{I_L} \tag{5}$$

The operation of the proposed control scheme of DVR under various cases is explained in the following subsection.

3.1. Case 1: Nominal grid voltage

The phasor diagram for nominal grid voltage condition is shown in Fig. 2(a). Under nominal grid voltage, the terminal voltage is made to lag the grid voltage by an angle δ and the DVR injects a voltage $\vec{V}^0_{cQ}$. The line current is exactly out of phase with the grid voltage to maintain unity power factor. The Fig. 2(d) shows that the DVR voltage leads the line current by a phase angle α_c. The complex power exchanged by the DVR under nominal grid voltage can be written as

$$S_c = \vec{V}^0_{cQ}(\vec{I_L}) \tag{6}$$

The real and reactive power exchanged by DVR under nominal grid voltage can be written as,

$$P^0_c = V^0_{cQ} I_L \cos\alpha_c \tag{7}$$

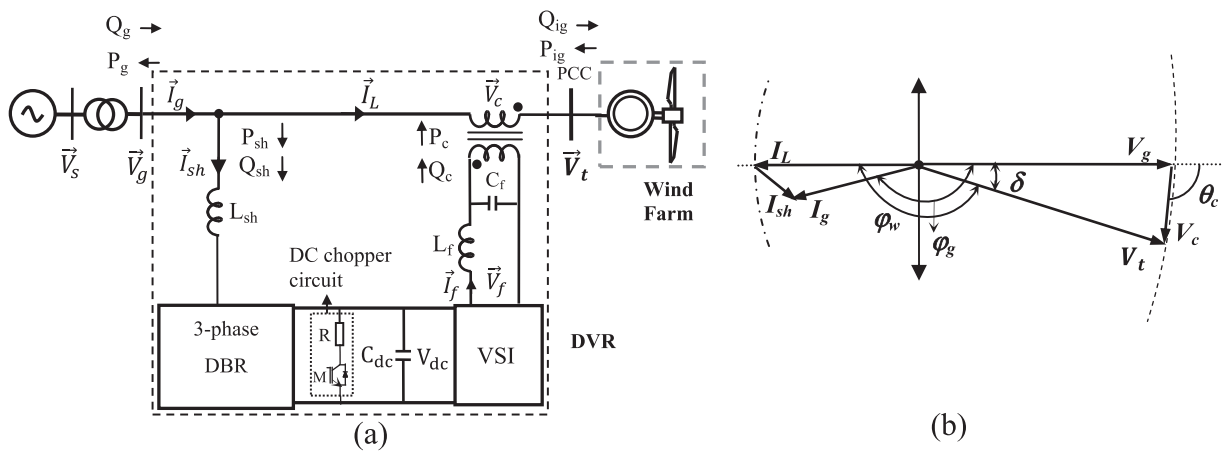

Fig. 1. (a) Schematic diagram of DVR in wind farm. (b) Phasor diagram of the proposed PA control.

$$Q_c^0 = V_{cQ}^0 I_L \sin\alpha_c \tag{8}$$

P_c^0 and Q_c^0 are the real and reactive power of DVR respectively under nominal grid voltage. It is inferred from (7) and (8) that the DVR should exchange certain real power with the grid to compensate the reactive power demanded by the FSWG.

The total real power (P_c) and reactive power (Q_c) exchanged by the DVR under nominal grid voltage condition, can be written as follows,

$$P_c = P_c^0 \tag{9}$$

$$Q_c = Q_c^0 \tag{10}$$

where P_c and Q_c are the total real and reactive power exchanged by the DVR under all conditions of grid voltage.

3.2. Case 2: Sag in grid voltage

The Fig. 2(b) shows the phasor diagram for sag in grid voltage wherein the DVR injects a voltage of $\vec{V}_c'$. From Fig. 2(b), the terminal voltage can be written as follows,

$$\vec{V}_t = \vec{V}_g' + \vec{V}_c' \tag{11}$$

where $\vec{V}_g'$ and $\vec{V}_c'$ denotes grid voltage and DVR voltage under sag in grid voltage.

Further the phasor $\vec{V}_c'$ can be resolved into two components as shown in Fig. 2(b) and can be written as follows,

$$\vec{V}_c' = \vec{V}_{cQ}' + \vec{V}_{c-sag}' \tag{12}$$

where $\vec{V}_{cQ}'$ is the component corresponding to reactive power compensation while $\vec{V}_{c-sag}'$ is the component corresponding to sag mitigation. The reactive power contributed (exchanged) due to $\vec{V}_{c-sag}'$ will be zero since the $\vec{V}_{c-sag}'$ is always in anti-phase (180°) with respect to the current $\vec{I}_L$ as shown in Fig. 2(e). The real and reactive power corresponding to sag mitigation is given by,

$$P_{c-sag}' = V_{c-sag}' I_L \cos 180 = -V_{c-sag}' I_L \tag{13}$$

$$Q_{c-sag}' = V_{c-sag}' I_L \sin 180 = 0 \tag{14}$$

Here, P_{c-sag}' and Q_{c-sag}' are the real and reactive components of power for mitigating sag.

The negative sign in (13) indicates that DVR absorbs real power during voltage sag condition. Further, the voltage component $\vec{V}_{cQ}'$ (which is primarily the reactive power compensation component of DVR) remains unchanged with varying grid voltage. Thus the real and reactive power exchanged due to $\vec{V}_{cQ}'$ are the same as in nominal grid conditions (Eqs. (7) and (8)). This is because the impedance and the phase of the generator terminal voltage are held constant (as explained earlier). Therefore the total real and reactive power exchanged by the DVR under grid voltage sag can be written as,

$$P_c' = P_{c-sag}' + P_{cQ}' \tag{15}$$

$$Q_c' = Q_{c-sag}' + Q_{cQ}' = Q_{cQ}' \tag{16}$$

Thus, the total real power component of the DVR under simultaneous sag mitigation and reactive power compensation depends on both the sag compensation component and the reactive power compensation component of DVR. Whereas, the reactive power component of the DVR depends only on reactive power compensating component since reactive power corresponding to sag mitigation is zero (14).

3.3. Case 3: Swell in grid voltage

The phasor diagram corresponding to grid voltage swell is given in Fig. 2(c) where the terminal voltage lags the grid voltage at an angle δ and DVR injects voltage of magnitude V_{cQ}'' at a phase angle θ_c''. From Fig. 2(c), the terminal voltage under grid voltage swell can be written as follows,

$$\vec{V}_t = \vec{V}_g'' + \vec{V}_c'' \tag{17}$$

where $\vec{V}_g''$ corresponds to swell in grid voltage and $\vec{V}_c''$ corresponds to voltage injected by DVR under swell in grid voltage.

The phasor $\vec{V}_c''$ of DVR can be resolved as follows,

$$\vec{V}_c'' = \vec{V}_{cQ}'' + \vec{V}_{c-swell}'' \tag{18}$$

where $\vec{V}_{c-swell}''$ is the voltage component corresponding to swell mitigation and $\vec{V}_c''$ is the total voltage injected by DVR under grid voltage swell.

The reactive power contributed (exchanged) due to $\vec{V}_{c-swell}'$ will be zero since the $\vec{V}_{c-swell}'$ is always in in-phase (0°) with respect to the current $\vec{I}_L$ as shown in Fig. 2(f). The real and reactive power corresponding to swell mitigation is given by,

$$P(c-swell)'' = V(c-swell)'' I_L cos 180 = V(c-swell)'' I_L \tag{19}$$

$$Q_{c-swell}'' = V_{c-swell}'' I_L I_L \sin 0 = 0 \tag{20}$$

Therefore the total real and reactive power exchanged by the DVR under grid voltage swell along with reactive power compensation can be written as,

$$P_c'' = P_{c-swell}'' + P_{cQ}'' \tag{21}$$

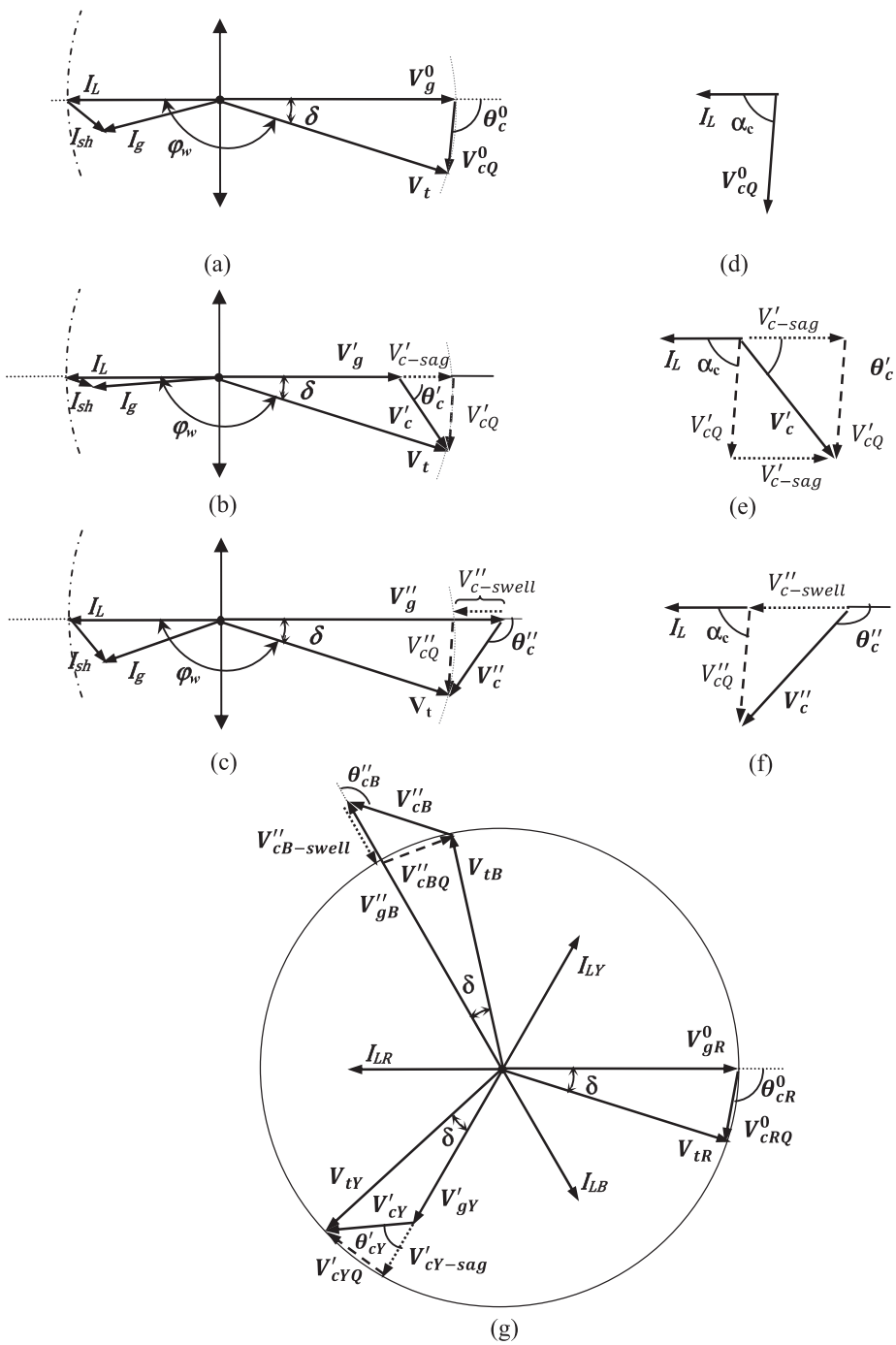

Fig. 2. Phasor diagram representation of Phase Angle control of DVR under different grid voltage conditions and DVR voltage vs line current (a), (d) nominal (b), (e) symmetrical sag and (c), (f) symmetrical swell in grid voltage (g) unsymmetrical grid voltage.

$$Q_c'' = Q_{c-swell}'' + Q_{cQ}'' = Q_{cQ}'' \tag{22}$$

The total real power of DVR depends on swell mitigation and reactive power compensation components whereas the total reactive power depends only on the reactive power compensation component since the reactive power component of swell is zero (20). Thus the reactive power compensating component remains fixed irrespective of variation in grid voltage since $\vec{V}_{cQ}^{0} = \vec{V}_{cQ}' = \vec{V}_{cQ}''$. Further the current through the shunt converter $\vec{I}_{sh}$ increases during swell due to increase in demand of real power (Fig. 2(c)) and reduces during sag due to decrease in demand of real power required by DVR as shown in Fig. 2(b). During sag, the DVR conveys the real power to be dissipated in the braking resistor of the dc chopper circuit to maintain the power balance.

3.4. Case 4: Unsymmetrical grid voltage

The case of unsymmetrical grid voltage is considered with a nominal voltage in R-phase, sag in Y-phase and swell in B-phase. The Fig. 2(g) shows the phasor diagram with 'PA' control implemented under unsymmetrical grid voltage condition. Although the grid voltage magnitude is different at each phase, the phase angle between the grid and terminal voltage remains constant at 'δ'. The total power exchanged by the DVR is the sum of powers exchanged at each phase.

For the R-phase with nominal voltage similar to the case 1 (Fig. 2 (a) and (d)), the real and reactive power exchanged are given by

$$P_{cR}^{0} = V_{cRQ}^{0} I_{LR} \cos\alpha_{cR} \tag{23}$$

$$\text{and } Q_{cR}^{0} = V_{cRQ}^{0} I_{LR} \sin\alpha_{cR} \tag{24}$$

where 'α_{cR}' is the phase angle between the DVR voltage and line current for R-phase. For the Y-phase with a voltage sag, similar to the case-2 (Fig. 2 (b) and (e)), the real and reactive power exchanged by DVR at Y-phase under sag in grid voltage are given by

$$P'_{cY} = P'_{cY-sag} + P'_{cYQ} \tag{25}$$

$$\text{and } Q'_{cY} = Q'_{cY-sag} + Q'_{cYQ} = Q'_{cYQ} \tag{26}$$

It can be noted that the Y-phase total compensation is the combination of sag mitigation and reactive power compensation by DVR. Similarly, for the B-phase with grid voltage swell, the real and reactive power exchanged by DVR are given by:

$$P''_{cB} = P''_{cB-swell} + P''_{cBQ} \tag{27}$$

$$\text{and } Q''_{cB} = Q''_{cB-swell} + Q''_{cBQ} = Q''_{cBQ} \tag{28}$$

This is similar to case-3 (Fig. 2 (c) and (f)) where the total compensation is the sum of swell mitigation and reactive power compensation.

The total real and reactive power exchanged by DVR under unsymmetrical grid voltage are given as:

$$P_c = P_{cR}^{0} + P'_{cY} + P''_{cB} \tag{29}$$

$$Q_c = Q_{cR}^{0} + Q'_{cY} + Q''_{cB} \tag{30}$$

Thus even under unsymmetrical grid voltage conditions, the terminal voltage and also the reactive power support to the wind generator can be maintained by simultaneously mitigating the sag or swell considering individual phases of grid.

Thus, it is inferred from the analysis that during nominal grid voltage and also under swell in grid voltage, DVR needs to inject certain real power to the grid to compensate the reactive power demand of FSWG. Therefore the real power to be injected by the DVR can be availed from grid through the shunt converter (DBR). Thus the real power delivered by the shunt converter to the DVR circulates between the shunt converter and the DVR to facilitate the injection of reactive power demanded by FSWG. Ideally the real power delivered through the shunt converter should be equal to the real delivered to the grid by the DVR considering zero losses. However there may be a small percentage of loss in switching devices, LC filter of DVR. Thus the PA control scheme maintains the steady state operation of FSWG irrespective of grid voltage variations and thus the real power generated by FSWG is extracted.

The real and reactive power exchanged by DVR for varying grid voltage are given in Fig. 3 corresponding to the practical wind farm data given in Table 1A (Appendix A). The real power component corresponding to the sag/swell mitigation is varying based on grid voltage whereas the real power is negative during sag conditions and positive during swell condition as shown in Fig. 3. Further the real power component corresponding to reactive power compensation is constant irrespective of grid voltage variation. Thus the total real power exchanged by DVR varies whereas the total reactive power exchanged by DVR remains constant under the grid voltage variation. The operating region of DVR under various grid voltage is explored graphically in the upcoming sub-section.

3.5. Operating region of DVR with phase angle control (Graphical Analysis)

To analyse the operating region of DVR with the proposed control, the following expressions are derived.

The complex power of the DVR can be obtained as follows (Fig. 1b),

$$S_c = \vec{V_c}(\vec{I_L})^* \tag{31}$$

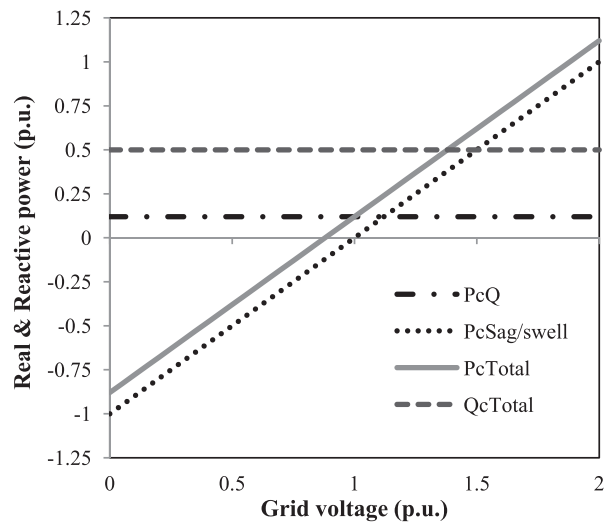

Fig. 3. Variation of real and reactive power exchanged by DVR under grid voltage variation.

By substituting (2) and (5) in (31), the real and reactive power of DVR under steady state are given by

$$P_c = \frac{V_t^2}{Z} cos\varphi_w - V_g I_g cos\varphi_g + V_g I_{sh} cos\varphi_{sh} \tag{32}$$

$$Q_c = \frac{V_t^2}{Z} sin\varphi_w + V_g I_g sin\varphi_g - V_g I_{sh} sin\varphi_{sh} \tag{33}$$

whereas φ_g is the angle between grid voltage and grid current and φ_{sh} is the angle between grid voltage and shunt current. By solving (32) and (33), the following expression can be obtained.

$$\left(P_c - \frac{V_t^2 cos\varphi_w}{Z}\right)^2 + \left(Q_c - \frac{V_t^2 sin\varphi_w}{Z}\right)^2 = \left(\frac{V_t V_g}{Z}\right)^2 \tag{34}$$

Eq. (34) represents a circle with the centre at $\left(\frac{V_t^2}{Z} cos\varphi_w, \frac{V_t^2}{Z} sin\varphi_w\right)$. The coordinates represent the real and reactive power exchanged by the wind farm whereas $\left(\frac{V_g V_t}{Z}\right)^2$ is the radius of the circle.

The operating region of DVR with PA control is explained in this section. Using the circle Eq. (34), the operating region of DVR connected to wind generator can be obtained as shown in Fig. 4. The specifications pertaining to a practical wind farm of 2 MW FSWG (in Appendix A) are used in plotting the characteristics of Fig. 4(a), (b) respectively. The Fig. 4(a) shows a set of concentric circles with the centre 'A' for various grid voltage magnitudes. The coordinates of the circles $\left(\frac{V_t^2}{Z} cos\varphi_w, \frac{V_t^2}{Z} sin\varphi_w\right)$ represents the real power delivered (−ve) and reactive power absorbed (+ve) by the wind farm respectively. The circle with centre 'D' as origin represents the operating region of the DVR while the radius represents the VA rating 'S_c' of the DVR. The concentric circles drawn for various grid voltages are mentioned from P_1 to P_5 as shown in the Fig. 4(a).

The apparent power rating of the DVR is represented as S_c and it is considered that the available DVR in wind farm is fully rated to wind generator rating for FRT. The radius with 1 p.u. of the circle S_c represents the VA rating of the DVR in Fig. 4(a) and (b) respectively. The horizontal line 'AB' denotes the constant reactive power as shown in Fig. 4(a). The intersecting points of the grid voltage circles (P_1 to P_5) with line 'AB' define the DVR operating points (V_1 to V_5) for various grid voltages. The operating points V_1-V_3 corresponds to grid voltage sag and V_4 corresponds to nominal grid voltage and V_5 corresponds to grid voltage swell. From the operating points of DVR (V_1 to V_5), it is observed that the DVR facilitates a constant reactive power under a range of grid voltage. However the real power exchanged by the

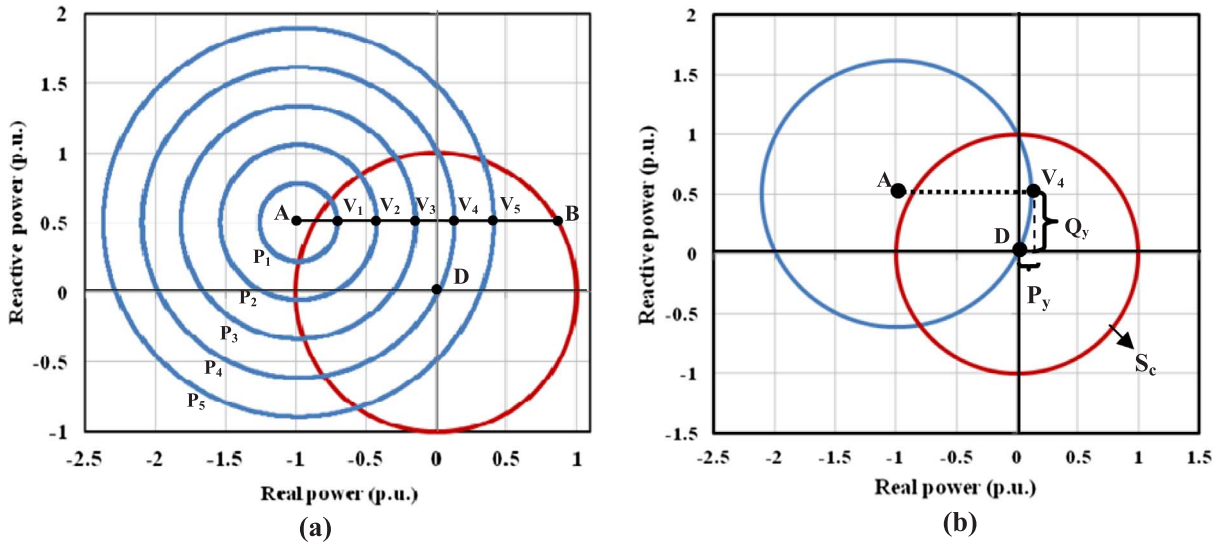

Fig. 4. Operating region of wind generator and DVR corresponding to (a) various grid voltages and (b) nominal grid voltage.

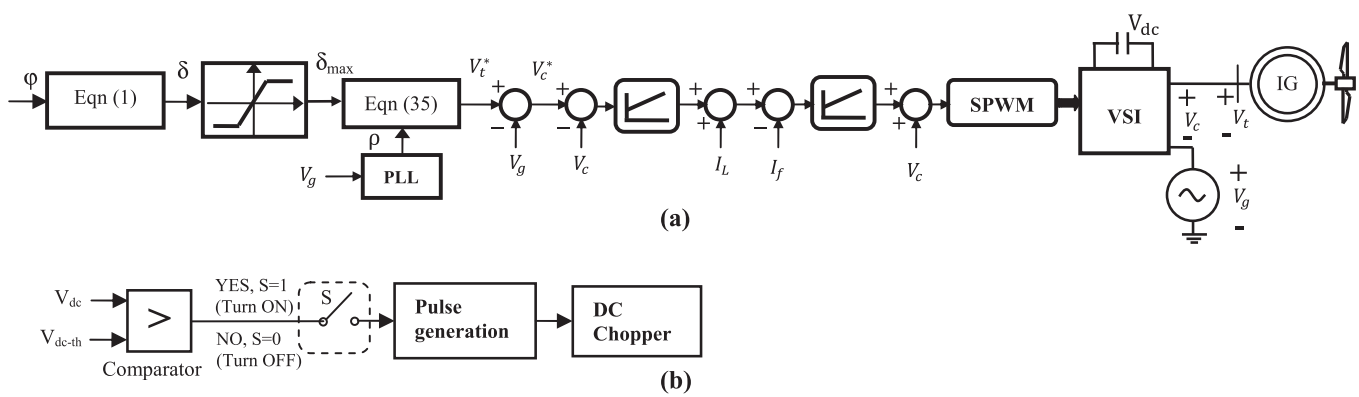

Fig. 5. Control scheme (a) phase ANGLE control in DVR and (b) DC chopper unit.

compensator varies according to the grid voltage sag/swell. For the grid voltage sag (V_1-V_3), the DVR operating points lies in the second quadrant of the operating region of DVR. However, during nominal operating conditions and also under swell in grid voltage, the operating point lies in first quadrant. Therefore the DVR absorbs (negative) and delivers (positive) the real and reactive power respectively under grid voltage sag. During nominal and swell conditions in grid voltage, the DVR delivers both real and reactive power.

The Fig. 4(b) shows the operating region of circle 'P_4' corresponding to nominal grid voltage and DVR. The reactive power line intersects the circle P_4 at operating point 'V_4' and correspondingly the DVR should inject a real power of 'P_y' and reactive power of 'Q_y'. Therefore under nominal grid voltage, to inject a reactive power of 'Q_y', the DVR should inject a real power of 'P_y' to maintain the steady state operation of the system which is also explored in the phasor diagram analysis. The detailed explanation on power exchanged by DVR under various conditions is described in the Section 5. Thus the DVR with 'Phase Angle' control can be operated to provide a constant reactive power and also mitigate the effects of sag/swell in grid voltage thus protecting the wind generator.

4. Implementation of phase angle control in DVR

The generation of reference signals for the DVR based on Phase Angle control is discussed in this section. The double closed loop inverter control is implemented in all the three phases of the DVR as shown in Fig. 5. The impedance phase angle φ_w is a known parameter for a given wind power generator and hence the angle 'δ' can be obtained from (1). A limiter is implemented to limit the phase angle δ to δ_{max} in order to avoid overloading of the DVR (for partially rated) using Eq. (35). The SRF-PLL is employed to maintain synchronization between the grid and DVR. The desired phase angle of the terminal voltage reference signal is computed from (1) and the reference for the terminal voltage is generated from the following equation,

$$V_t^* = V_t \sin(\rho(t) + \delta) \tag{35}$$

where ρ(t) is obtained using PLL.

The difference between the reference signal of V_t^* and grid voltage is processed in the voltage control loop. The inner current control loop and outer voltage control loop generate the modulating signals to be fed to the SPWM block for generating the switching pulses for DVR.

The control logic for the dc chopper circuit is given in Fig. 5(b). To maintain the dc link voltage within the limit, V_{dc} voltage is sensed and compared with the threshold. If $V_{dc} > V_{dc\text{-}th}$, the logic switch 'S' is closed and pulse is generated for the switch 'M' (shown in Fig. 1) and thus the excess real power is dissipated in the braking resistor in order to maintain the nominal operation of wind generator. If $V_{dc} < V_{dc\text{-}th}$, the dc chopper circuit is maintained inactive.

5. Results and discussion

The proposed control strategy is validated in simulations and experiments under grid voltage sag/swell. The source convention is followed for grid and DVR and the load convention is followed for wind

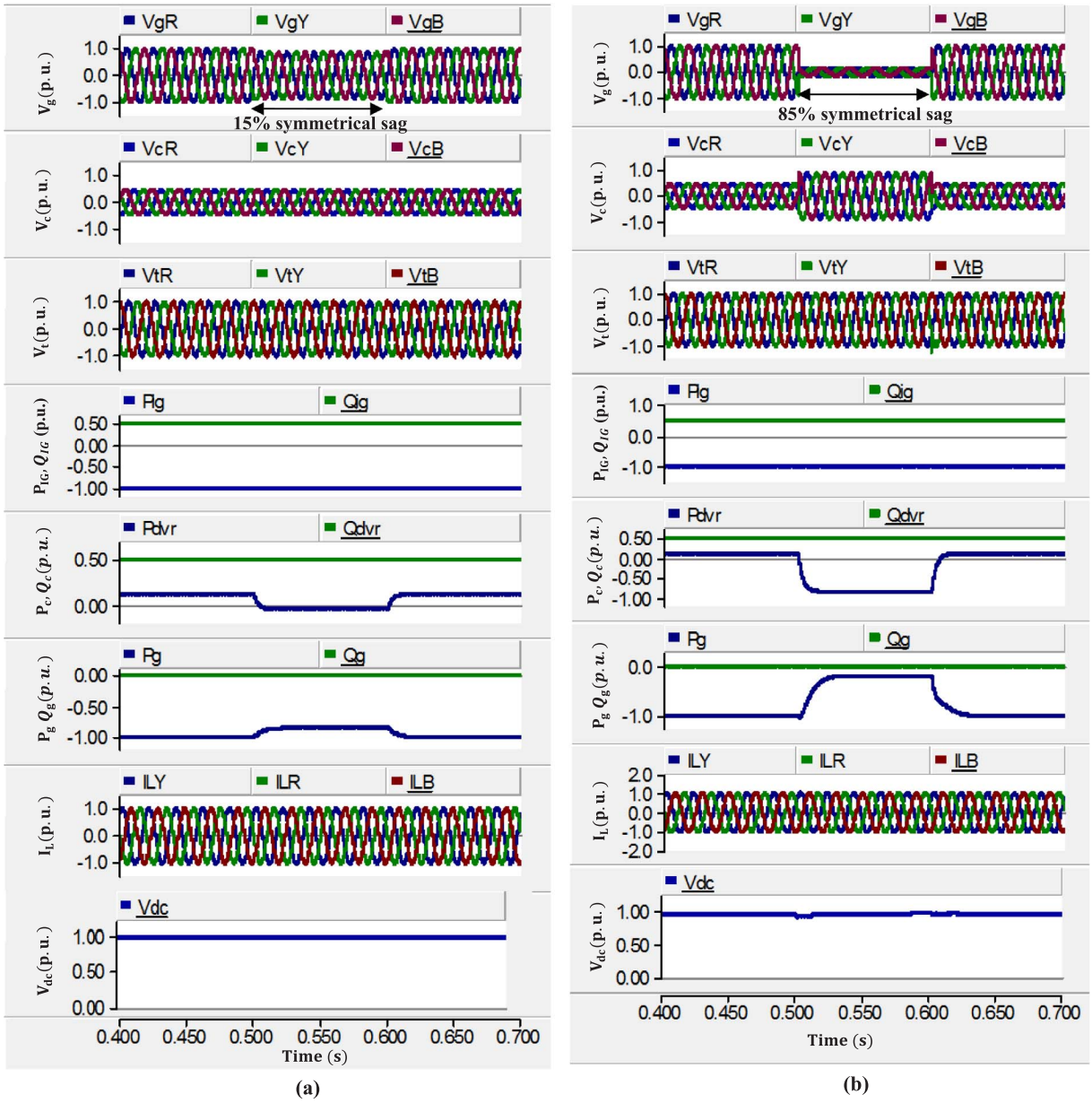

Fig. 6. Simulation results (a) system response under 15% symmetrical sag and (b) system response under 85% symmetrical sag in grid voltage.

generator and shunt converter as mentioned earlier. The system parameters considered for simulation and experiment are given in Table 1A (Appendix A).

5.1. Simulation results

The simulation is carried out in PSCAD/EMTDC software to observe the performance of the proposed control strategy under various grid voltage conditions. The SPWM is implemented with a carrier frequency of 5 kHz for pulse generation to DVR. A fixed speed induction generator of 2 MW power rating is considered in the simulation study. The performance of the proposed control strategy is tested under four cases: (i) Case 1: Nominal grid voltage (ii) Case 2: Symmetrical sag (iii) Case 3: Symmetrical swell in grid voltage and (iv) Case 4: Unsymmetrical Grid voltage.

5.1.1. Case 1: Nominal grid voltage

With a nominal grid voltage, the phase angle between grid and the generator voltage is computed (as $\delta = 27^\circ$ calculated from (1)) and is maintained by commanding the DVR to inject a voltage of 0.45 p.u.($V_{c\text{-}rms}$ = 179.15 V) at a phase angle of $\theta_c = 98^\circ$ with respect to grid voltage. As a consequence, the DVR supplies a reactive power of 0.5 p.u. to the wind generator while it also supplies a real power of 0.12 p.u. to the grid (Fig. 6 (a) and (b)). Here it is notable that the real power supplied by DVR gets reflected as a demand to the grid via the diode bridge rectifier (DBR). Thus this real power (0.12 p.u.) essentially comes from the grid through the DBR and then DVR supplies it to the grid at the series transformer.

5.1.2. Case 2: Sag in grid voltage

A 15% sag in grid voltage is introduced during t = 0.5 s to 0.6 s and the corresponding dynamic response is shown in Fig. 6(a). The voltage injected by DVR changes to 0.455 p.u. with phase angle $\theta_{c\text{-}sag} = 85^\circ$ with respect to grid voltage to compensate the sag and reactive power to be supplied to the wind generator. During grid voltage sag, the real power absorbed by the grid reduces and thus the DVR absorbs a part of real power as shown in Fig. 6(a). Since the DVR maintains a constant terminal voltage, the real and reactive power exchanged by the wind

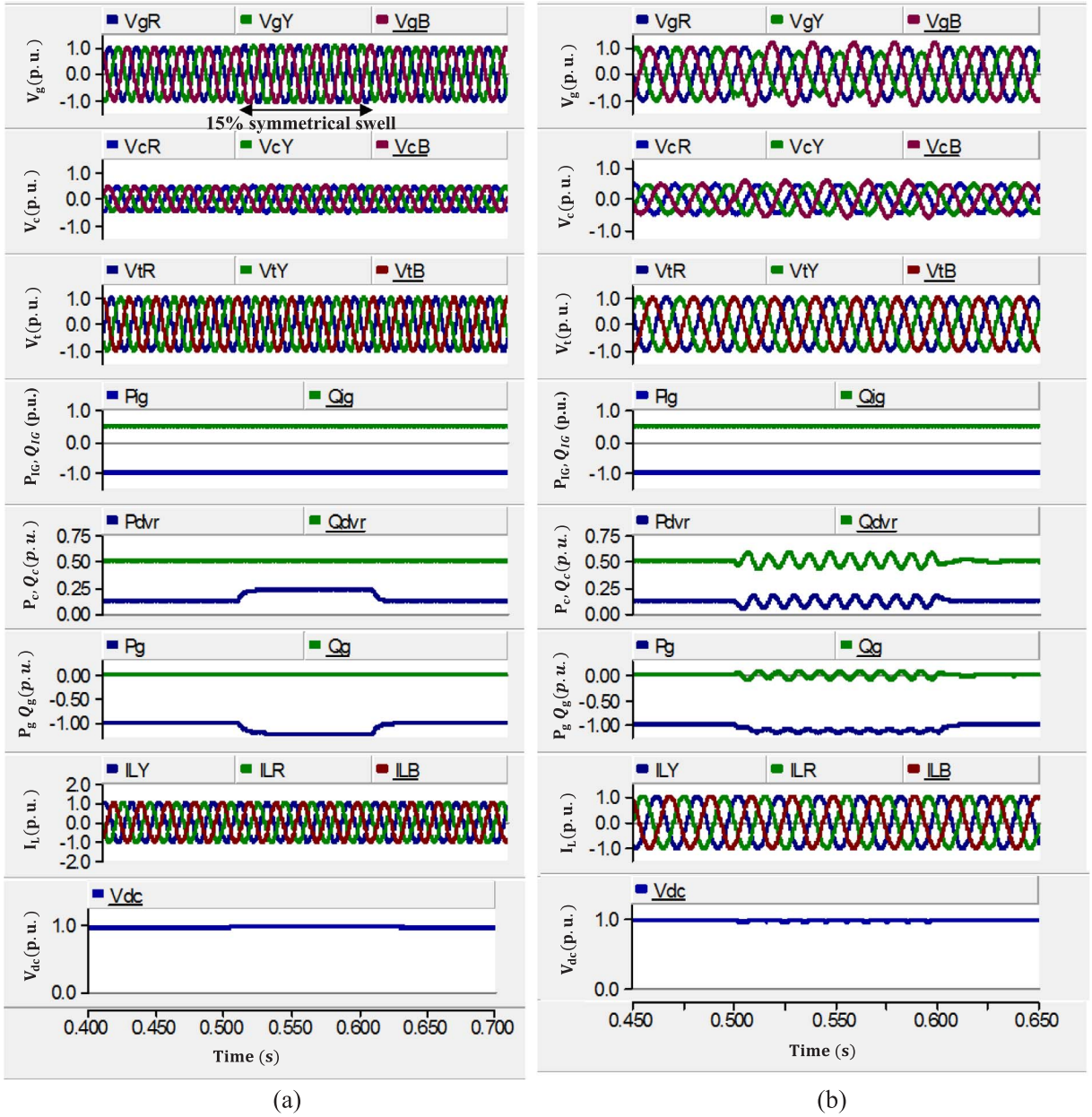

Fig. 7. Simulation results (a) system response under 15% symmetrical swell, (b) system response under unsymmetrical grid voltage with 15% sag in Y-phase and 15% in B-phase grid voltage.

generator maintained constant (Fig. 6(a)).

As per IEGC grid code for wind farms, the wind generators should be connected to grid till 85% sag in grid voltage as given in [2]. Therefore the case of 85% dip in grid voltage is also tested to validate the efficacy of the scheme. A symmetrical sag of 85% is introduced at t = 0.5 s until t = 0.6 s following which the DVR injects a voltage of 0.87 p.u. at an angle 33° with respect to grid voltage to mitigate sag in grid voltage and to compensate the reactive power requirement of wind generator simultaneously. Fig. 6(b) shows that the DVR maintains a constant supply of reactive power to the wind generator even under deep sag condition. Here again, the DVR absorbs the balance of real power from wind generator and dissipates the same through the braking resistor in the dc-chopper circuit and thus the dc-link voltage is maintained as shown in Fig. 6(b). Thus the 'PA' control facilitates simultaneous sag mitigation and reactive power compensation.

5.1.3. Case 3: Swell in grid voltage

A 15% swell in grid voltage is introduced during t = 0.5 s to 0.6 s and the corresponding dynamic response is shown in Fig. 7(a). The DVR injects a voltage of 0.54 p.u. at an angle of 124° with respect to grid voltage to compensate the swell and reactive power to the wind generator. During grid voltage swell, the grid absorbs excess real power whereas the power delivered by wind generator is fixed, hence the balance of real power is to be delivered by DVR to maintain the equilibrium operation of the system as shown in Fig. 7(a). Further the DVR supplies constant reactive power to the wind generator by compensating for the swell in grid voltage while the terminal voltage is maintained at V_t = 1.0 p.u.

Fig. 8(a) show the phase relationship among the grid, DVR and generator terminal voltages and line current under 85% sag in grid voltage. The grid voltage V_{gR} leads the terminal voltage V_{tR} by an angle δ = 27° as shown in Fig. 8(a). The line current is exactly out of phase irrespective of sag in grid voltage and thus the wind generator

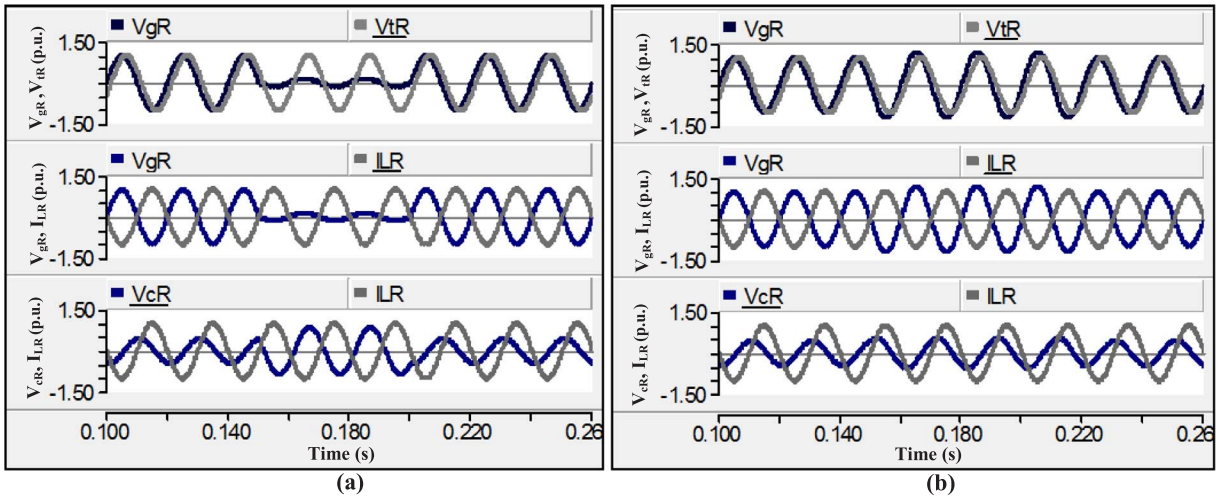

Fig. 8. Phase angle relation between voltage and current (a) during 85% symmetrical sag and (b) during 15% swell in grid voltage.

Table 1
Real and reactive power at various grid voltage conditions in the system-simulation.

Grid voltage	Grid		DVR		Wind generator		Shunt converter (DBR)	
	P_g (p.u.)	Q_g (p.u.)	P_c (p.u.)	Q_c (p.u.)	P_w (p.u.)	Q_w (p.u.)	P_{sh} (p.u.)	Q_{sh} (p.u.)
Nominal – 1.0 p.u.	−1.0	≈ 0	+0.12	+0.5	−1.0	+0.5	+0.12	≈ 0
Sag(15%) – 0.85 p.u.	−0.85	≈ 0	−0.05	+0.5	−1.0	+0.5	+0.10	≈ 0
Swell(15%) – 1.15 p.u.	−1.15	≈ 0	+0.29	+0.5	−1.0	+0.5	+0.14	≈ 0
Source convention (Grid and DVR)			Load convention (Wind Generator and Shunt converter (DBR))					
P or Q is +ve = Supplying P or Q is −ve = Absorbing			P or Q is +ve = Absorbing P or Q is −ve = Supplying					

Table 2
Numerical data of simulation and experiment.

	DVR rating (p.u.)	Event	V_g (p.u.)	δ (°)	θ_c (°)	Vc (p.u.)	Φ_c (°)
Simulation	1	Nominal	1	27	98	0.45	82
		15% Sag	0.85	27	85	0.445	95
		85% Sag	0.15	27	33	0.87	147
		15% Swell	1.15	27	124	0.54	56
Experiment	0.273	Nominal	1	12	102	0.22	46
		15% Sag	0.85	12	68	0.24	72
		15% Swell	1.15	12	125	0.252	22

maintains unity power factor with respect to the grid. The magnitude and phase angle of DVR voltage change with the sag in grid voltage as shown in Fig. 8(a). Fig. 8(b) show the phase relationship among the grid, DVR and generator terminal voltages and line current under 15% sag in grid voltage. The grid voltage V_{gR} leads the terminal voltage V_{tR} by an angle δ = 27° as shown in Fig. 8 (b). The line current is exactly out of phase irrespective of swell in grid voltage and thus the wind generator maintains unity power factor with respect to the grid. The magnitude and phase angle of DVR voltage change with swell in grid voltage Fig. 8(b). Table 1 shows the real and reactive power exchanged in the system under nominal, sag(15%) and swell(15%) in grid voltage. Further the wind generator real and reactive power are maintained balanced under various grid voltage conditions with the power exchanged by the DVR, grid and shunt converter (DBR) as given in Table 1.

5.1.4. Case 4: Unsymmetrical grid voltage

The performance of the system under unsymmetrical grid voltage with 'PA' control is given in Fig. 7(b) wherein a 15% sag at Y-phase and a 15% swell at B-phase are introduced for a duration of t = 0.5–0.6 s. Due to unsymmetrical grid voltage condition, the power exchanged by the grid consists of double frequency content and in order to compensate the sag and swell simultaneously (unsymmetrical grid voltage), the voltage injected by DVR is also unsymmetrical and thus the total real and reactive power exchanged by DVR also consists of double frequency content as shown in the Fig. 7(b). However the reactive power absorbed and the real power injected by the wind generator are at steady values (due to constant speed operation) irrespective of unsymmetrical grid voltage. The terminal voltage is maintained constant at V_t = 1.0 p.u. as shown in Fig. 7(b) while the dc-link voltage is maintained below the threshold value as shown in Fig. 7(b). Thus the proposed 'PA' control facilitates a steady operation of constant real power (and reactive power) from (and to) the wind generator to the grid even under unsymmetrical grid voltage condition. Table 2 gives the details of voltage injection by DVR under sag, swell and nominal grid voltage conditions.

5.2. Experimental results

The performance of the proposed 'PA' control scheme is verified using a prototype model of DVR with a rating of 0.34 kVA (0.273 p.u.) available in laboratory through experiments. A separately exited 1hp dc motor is employed for driving a 0.75 kW induction machine as the wind power generator. A three phase auto transformer is connected in between the grid and the DVR to introduce voltage sag/swell. The dc link of the inverter is charged through a three phase diode bridge rectifier from the grid. The LEM sensors are used to sense the voltages and currents and the op-amp (IC741) is utilized for signal conditioning circuit. The control strategy is implemented in the ALTERA Cyclone-II FPGA digital controller. The SRF-PLL is implemented for grid

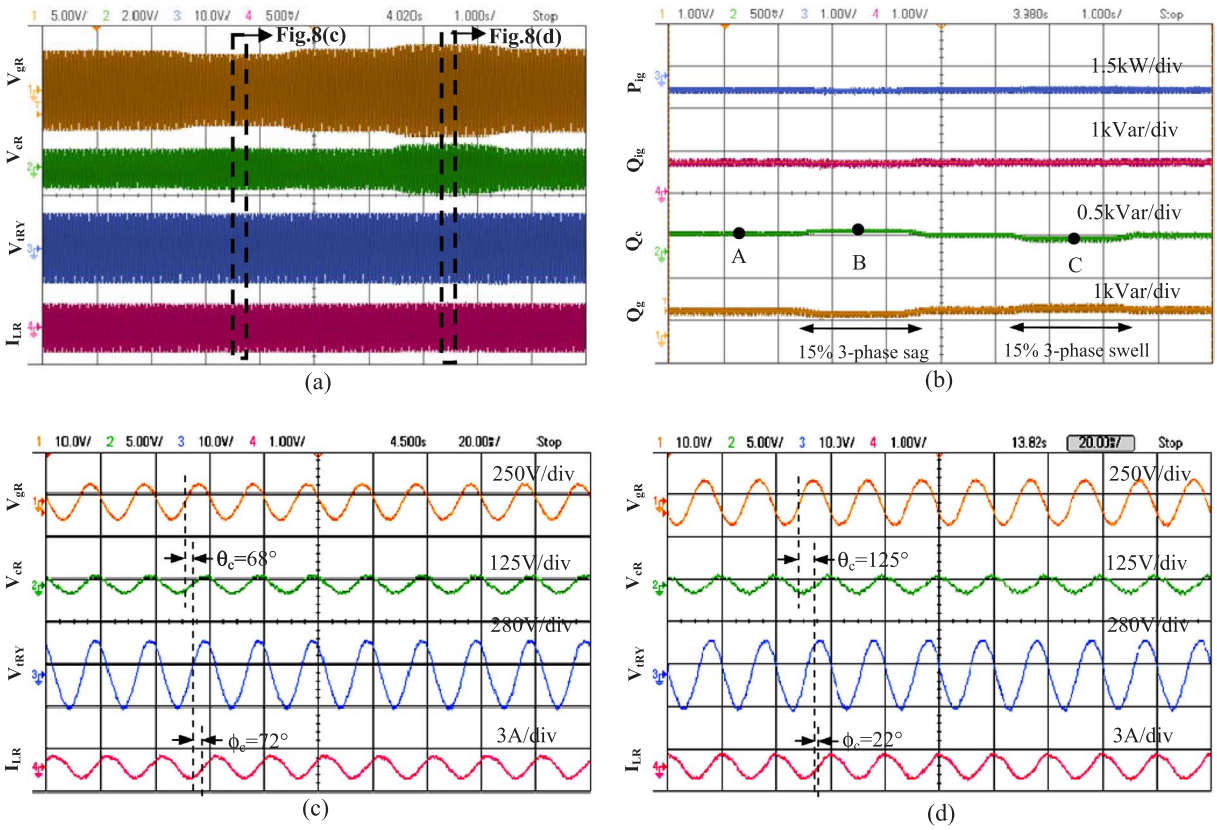

Fig. 9. System response under symmetrical grid voltage sag/swell – (a) Grid R-phase voltage, V_{gR}(110 V/div), DVR R-phase voltage, V_{cR}(50 V/div), terminal line-line voltage, V_{tRY}(190 V/div), line current, I_{LR}(3A/div), (b) real power of IG and reactive power exchange during 15% sag and 15% swell in grid voltage, real power of IG, P_{ig} (kW), reactive power of IG, Q_{ig}(KVar), DVR, Q_{DVR}(KVar), grid, Q_g(KVar), (c) expanded view of voltages and current during 15% sag and (d) Expanded view of voltages and current during 15% swell in grid voltage.

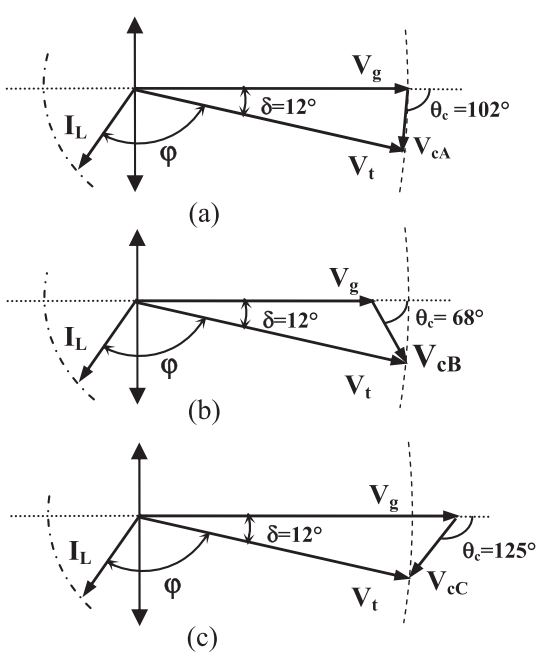

Fig. 10. Phasor diagram under three cases of grid voltage corresponding to experimental results (a) under nominal grid voltage, (b) under symmetrical sag and (c) under symmetrical swell.

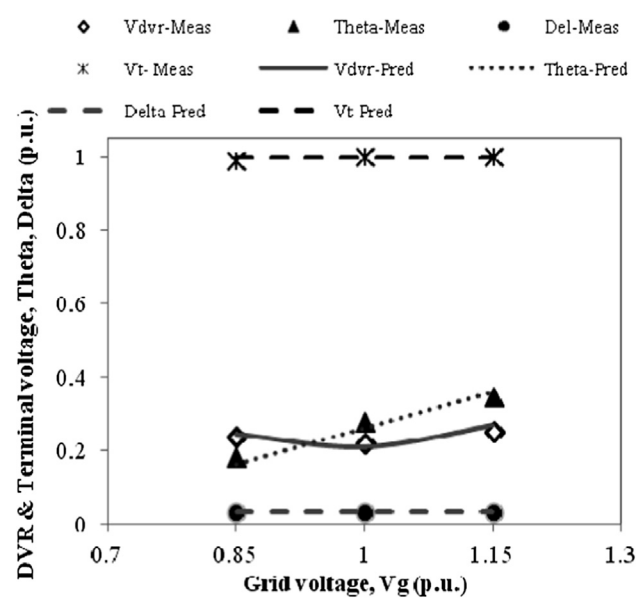

Fig. 11. Variation of DVR and terminal voltage, DVR phase angle theta(θ_c) and delta(δ) with respect to grid voltage.

synchronization and a unipolar SPWM technique is employed with 5 kHz switching frequency.

Since the DVR rating of the laboratory set up is only fractionally rated compared to the generator rating, the DVR facilitates only a part of reactive power to the wind generator and also the phase angle δ should be limited based on DVR rating to avoid overloading of DVR which can be obtained from (36) as follows,

$$\delta_{max} = \cos^{-1}\left(\frac{V_t^2 + V_g^2 - V_{c(max)}^2}{2V_g V_t}\right) \tag{36}$$

Thus a limiter is used in control strategy to avoid the phase angle δ to

exceed δ_{max}.

From (36), the maximum possible phase angle could to be maintained for the laboratory set up is $\delta_{max} \leq 15^\circ$ and the phase angle is chosen as $\delta = 12^\circ$ in experiment to avoid overloading during sag/swell in grid voltage. The experimental results with 'PA' control in DVR under grid voltage sag/swell are shown in Fig. 9(a)–(d). Under nominal grid voltage, the terminal voltage is maintained with phase angle $\delta = 12^\circ$ with the grid voltage whereas the DVR injects 48.2 V (0.22 p.u.) at an angle of 102° with respect to grid voltage as shown in Fig. 10(a). This facilitates to supply a part of reactive power to the generator whereas the grid supplies the remaining reactive power demanded by the generator. To facilitate simultaneous operation of reactive power supply and to maintain constant terminal voltage at 1.0 p.u., the DVR has to inject a certain real power during nominal grid voltage (as discussed in analysis) which is absorbed from grid through the diode bridge rectifier. However the absorbed real power through DBR is delivered back to the grid through DVR and thus the circulating real power facilitates the DVR to supply reactive power to the generator by maintaining the terminal voltage at nominal level. The Fig. 9(a) and (b) show the real and reactive power delivered under nominal grid voltage with 'PA' control.

The efficacy of the 'PA' control under 15% symmetrical sag is observed in Fig. 9(a)–(c) wherein the phase angle between the grid and terminal voltage is maintained constant at $\delta = 12^\circ$. The voltage injected by DVR changes to 52.2 V (0.24 p.u.) at an angle 68° with respect to grid voltage to compensate the sag along with reactive power compensation. The corresponding phasor diagram is shown in Fig. 10(b). Under grid voltage sag the reactive power delivered by the grid reduces and hence the reactive power to be supported by DVR increases thus the sag is mitigated while the reactive power demanded by the generator is also met. The changes in phase angle of DVR under sag are shown in Fig. 9(c).

The performance of the 'PA' control is tested under swell by applying a 15% of symmetrical swell in grid voltage as shown in Fig. 9(a) and (b) whereas the phase angle δ is maintained constant at $\delta = 12^\circ$. The DVR injects a voltage of 55.44 V(0.252 p.u.) at an angle 125° with respect to grid voltage to compensate the swell along with reactive power support. The corresponding phasor diagram of swell event is shown in Fig. 10(c). The reactive power delivered by the grid increases under swell whereas the reactive power injected by DVR decreases to compensate the swell and thus the real and reactive power exchanged by IG is also maintained constant. Further the change in phase angle of DVR under sag is shown in Fig. 9(d).

Thus the terminal voltage is maintained constant at 1.0 p.u. with DVR under grid voltage sag/swell and thus the real and reactive power of generator are also maintained constant as shown in Fig. 9(a) and (b). The variation in the DVR voltage magnitude and phase angle under various grid voltage conditions are given in Table 2.

The predicted and experimental results are compared to validate the proposed control scheme (Fig. 11). The close agreement between the predicted and experimental results for the 0.75 kW SCIG setup demonstrates the efficacy of the proposed 'PA' control scheme.

6. Conclusions

This paper proposes a new concept of simultaneous reactive power supply and sag/swell mitigation with DVR installed in grid connected wind farms (fixed speed). The concept involves controlling the DVR in such a way that the magnitude of the generator voltage is maintained at 1.0 p.u. whereas the phase of the generator voltage is maintained at a predetermined value with respect to the grid voltage to address the dual issues of sag/ swell mitigation and reactive power support to the generator. A comprehensive analysis of the 'Phase Angle' control is presented and the boundaries of operation for simultaneous reactive power supply and sag/swell mitigation are illustrated. Simulations using PSCAD/EMTDC software and also experiments using a laboratory set up demonstrate the viability of the proposed control. The important points of the proposed "Phase Angle" control strategy are;

(1) A fixed phase difference is to be maintained between the generator terminal voltage and the grid voltage to ensure a constant reactive power supply to the generator running at a fixed speed.
(2) By maintaining a constant phase angle as cited above, simultaneous operation of reactive power compensation and sag/swell mitigation can be achieved.
(3) Better utilization of DVR is achieved when compared to other compensation methods without affecting the steady state operation of wind generator.
(4) The proposed control does not affect the active power delivered by wind generator to the grid.

Thus the proposed "Phase Angle" control strategy is effective for simultaneous reactive power compensation and sag/swell mitigation in DVR installed fixed speed wind farms.

Appendix A

(see Tables 1A and 1B).

Table 1A
System parameters.

Parameters	Practical wind farm	Laboratory setup
Rated active power	2 MW	0.75 kW
Rated voltage(line to line rms)	690 V	380 V
Stator resistance, R_s	0.0108 p.u.	0.0311 p.u.
Stator reactance, X_s	0.107 p.u.	0.081 p.u.
Rotor resistance, R_r	0.01214 p.u.	0.0566 p.u.
Rotor reactance, X_r	0.1407 p.u.	0.081 p.u.
Magnetizing reactance, X_m	4.4 p.u.	0.95 p.u.
Filter inductance	4 mH	3.8 mH
Filter capacitance	300 μF	240 μF
DVR VA rating	1 p.u.	0.273 p.u.

Table 1B
Nomenclature.

V, I	Voltage and current
φ, α_L	Impedance angle of wind generator, Line current angle
δ	Phase angle of generator voltage with respect to grid voltage
θ_c, Φ_c	Phase angle of voltage injected by DVR, power factor angle of DVR
P, Q, S	Real, reactive, complex power
Z	Impedance of wind farm
R, C	Resistance, capacitance
First subscripts	
g,t, max, sh, L,w	Grid, terminal, maximum, shunt, Line, wind generator
Superscripts	
$*, ', ''$	Reference, Sag, Swell

Appendix B. Supplementary material

Supplementary data associated with this article can be found, in the online version, at http://dx.doi.org/10.1016/j.ijepes.2018.03.016.

References

[1] The Global Wind Energy Council. GWEC's Global Wind Report; 2014.
[2] Central Electricity Regulatory Commission, Ministry of Power, Central Government of India, Central Electricity Authority (Grid Standards) Regulations, 2010. The Gazette of India; 2014.
[3] Tsili M, Papathanassiou S. A review of grid code technical requirements for wind farms. Renew Power Gener IET 2009;3(3):308–32.
[4] Park Chang-Hyun, Jang Gilsoo. Voltage quality assessment considering low voltage ride-through requirement for wind turbines. Transmiss Distrib 2016;10(16):4205–12.
[5] Heydari-doostabad Hamed, Khalghani Mohammad Reza, Khooban Mohammad Hassan. A novel control system design to improve LVRT capability of fixed speed wind turbines using STATCOM in presence of voltage fault. Int J Elect Power Energy Syst 2015;77:280–6.
[6] Muyeen SM. A combined approach of using an SDBR and a STATCOM to enhance the stability of a wind farm. IEEE Syst J 2015;9(3):922–32.
[7] Ramirez Dionisio, Martinez Sergio, Blazquez Francisco, Carrero Carmelo. Use of STATCOM in wind farms with fixed-speed generators for grid code compliance. Renewable Energy 2012;37:202–12.
[8] Wessels Christian, Hoffmann Nils, Molinas Marta, Fuchs Friedrich Wilhelm. StatCom control at wind farms with fixed-speed induction generators under asymmetrical grid faults. IEEE Trans Indust Electron 2013;60(7):2864–73.
[9] Mohammadpour Hossein Ali, Islam Md Moinul, Santi Enrico, Shin Yong-June. SSR damping in fixed-speed wind farms using series FACTS controllers. IEEE Trans Power Delivery 2016;31(1):76–86.
[10] Jiang Fei, Tu Chunming, Shuai Zhikang, Xiao Fan, Lan Zheng. Combinational voltage booster technique for fault ride-through capability enhancement of squirrel-cage induction generator. Electr Power Syst Res 2016;136:163–72.
[11] Firouzi, Gharehpetia Gevork B, Mozafari Seid Babak. Application of UIPC to improve power system stability and LVRT capability of SCIG-based wind farms. IET Gen Trans Distrib 2017;11(9):2314–22.
[12] Naderi Seyed Behzad, Negnevitsky Michael, Jalilian Amin, Hagh Mehrdad Tarafdar. Fault ride through improvement of fixed speed wind turbine using RC-FCL with its modified control strategy. In: Australasian Universities Power Engineering Conference- AUPEC; 2016.
[13] Firouzi M, Gharehpetian GB. Improving fault ride-through capability of fixed-speed wind turbine by using bridge-type fault current limiter. IEEE Trans Energy Convers 2013;28(2):361–9.
[14] Naderi Seyed Behzad, Negnevitsky Michael, Jalilian Amin, Hagh Mehrdad Tarafdar, Muttaqi Kashem M. Optimum resistive type fault current limiter: an efficient solution to achieve maximum fault ride-through capability of fixed-speed wind turbines during symmetrical and asymmetrical grid faults. IEEE Trans Ind Appl 2017;53(1):538–48.
[15] Qazi Sajid Hussain, Mustafa Mohd Wazir. Review on active filters and its performance with grid connected fixed and variable speed wind turbine generator. Renew Sustain Energy Rev 2016;57:420–38.
[16] Amutha N, Kalyan Kumar B. Improving fault ride-through capability of wind generation system using DVR. Elect Power Energy Syst 2013;46:326–33.
[17] Hussein Ahmed Abu, Ali Mohd Hasan. Comparison among series compensators for transient stability enhancement of doubly fed induction generator based variable speed wind turbines. IET Renew Power Gener 2015;10(1):116–26.
[18] Moghadasi Amirhasan, Sarwat Arif, Guerrero Josep M. A comprehensive review of low-voltage-ride-through methods for fixed-speed wind power generators. Renew Sustain Energy 2016;55:823–39.
[19] Leon E, Farias MF, Battaiotto PE, Solsona JA, Valla MI. Control strategy of a DVR to improve stability in wind farms using squirrel-cage induction generators. IEEE Trans Power Syst 2011;26(3):1609–17.
[20] Ramirez Dionisio, Martinez Sergio, Latero Carlos A, Blazquez Francisco, de Castro Rosa M. Low-voltage ride-through capability for wind generators based on dynamic voltage restorers. IEEE Trans Energy Convers 2011;26(1):195–203.
[21] Gaztanaga H, Bacha S. Fixed-speed wind farm operation improvement by using DVR devices. IEEE-Proceedings; 2007.
[22] Wessels Christian, Gebhardt Fabian, Fuchs Friedrich Wilhelm. Fault ride-through of a DFIG wind turbine using a dynamic voltage restorer during symmetrical and asymmetrical grid faults. IEEE Trans Power Electron 2011;26(3):807–15.
[23] Ibrahim Ahmad Osman, Nguyen Thanh Hai, Lee Dong-Choon, Kim Su-Chang. A fault ride-through technique of DFIG wind turbine systems using dynamic voltage restorers. IEEE Trans Energy Convers 2011;26(3):871–82.
[24] Jerin A Rini Ann, Kaliannan Palanisamy, Subramaniam Uma Shankar. Improved fault ride through capability of DFIG based wind turbines using synchronous reference frame control based dynamic voltage restorer. 70. ISA transactions: Elsevier; 2017. p. 465–74.
[25] Agalar Sener, Kaplan Yusuf Alper. Power quality improvement using STS and DVR in wind energy system. Renewable Energy 2017:1–10.
[26] Naderi Seyed Behzad, Negnevitsky Michael, Jalilian Amin, Hagh Mehrdad Tarafdar, Muttaqi Kashem M. Low voltage ride-through enhancement of DFIG-based wind turbine using DC link switchable resistive type fault current limiter. Int J Elect Power Energy Syst 2017;86:104–19.
[27] Badrzadeh Babak. Transient recovery voltages caused by capacitor switching in wind power plants. IEEE Proc industry appl soc annual meeting, October 2012.
[28] Study on power quality issues in grid connected wind farms and their remedial measures. C-WET report, March 2014. p. 34–6.
[29] Patil Hardik U. Harmonic Resonance in Power Transmission Systems due to the Addition of Shunt Capacitors M.S. Dissertation Arizona State University; 2015.
[30] Steurer M, Langston J, Anderson L, Suryanarayanan S, Meeker R, Ribeiro P. Voltage sensitivity to capacitor switching on an existing fixed speed induction generator wind farm. IEEE power engineering society general meeting, Tampa, FL, USA, June-2007.
[31] Nielsen JG, Blaabjerg F. A detailed comparison of system topologies for dynamic voltage restorers. IEEE Trans Ind Appl 2005;41(5):1272–80.
[32] Rau Abdul Mannan, Khadkikar Vinod. An enhanced voltage sag compensation scheme for dynamic voltage restorer. IEEE Trans Indust Electron 2015;62(5):2683–92.
[33] Akhmatov V. Analysis of dynamic behaviour of electric power systems with large amount of wind power Ph.D. Dissertation Lyngby (Denmark): Tech Univ; 2003.